Available online at www.sciencedirect.com

ScienceDirect

Energy Procedia 49 (2014) 2280 – 2289

Energy Procedia

SolarPACES 2013

Prediction of cloudiness in short time periods using techniques of remote sensing and image processing

Joaquín Alonso[a], Antonio Ternero[b], Francisco J. Batlles[a,]*, Gabriel López[c], Jorge Rodríguez[b], Juan I. Burgaleta[b]

[a]*Department of Chemistry and Physics, University of Almería, 04120 Almería, Spain*
[b]*Torresol Energy, O&M, S.A., Avda. Zugazarte 61, 48930 Getxo (Vizcaya), Spain*
[c]*Department of Electrical and Thermal Engineering, University of Huelva, 21004 Huelva, Spain*

Abstract

In this work we introduce a methodology which enables to predict the cloudiness in the short and medium termanywhere in the world. Satellite images (Meteosat of Second Generation) are used in combination with images from a sky camera (fisheye lens), showing a ground vision of the clouds, and using the real-time radiation measured on-site as a feedback and as a complement to the cloudiness. The methodology is based on the determination of cloud motion in the images. Obtaining cloud movement vectors from consecutive images, we are able to anticipate the displacement of the previously detected clouds, thus knowing the distribution of clouds in the future. The short-term forecast (less than 1 hour) and the medium-term forecast (up till 3 hours) have a rate of success of 80%. Aiming to have an accurate knowledge of the evolution of cloudiness in the short and medium-term (useful for CSP plant management) an interactive portal has been developed. The application is a user-friendly interface which shows three hours real-time forecasts refreshed each minute, along with useful information for the operation of the CSP plant like the DNI evolution, the original and processed image from satellite MSG-2 as well as that from sky camera. In the application 400 Wm^{-2} will be considered as the DNI threshold for the optimal operation for a CSP plant. The application has been tested and validated in two different locations: University of Almería (Almería, Spain) and Gemasolar Central Tower Plant (Fuentes de Andalucía, Spain) and it is going to be installed in Valle 1 and 2 Parabolic Trough Plant (San José del Valle, Spain).

Selection and peer review by the scientific conference committee of SolarPACES 2013 under responsibility of PSE AG.
Final manuscript published as received without editorial corrections.
Keywords: forecast, cloudiness, remote sensing, Meteosat Second Generation, sky cameras

* Corresponding author. Tel.: +34-950-015914; fax: +34-950-015477.
E-mail address: fbatlles@ual.es

Selection and peer review by the scientific conference committee of SolarPACES 2013 under responsibility of PSE AG.
Final manuscript published as received without editorial corrections.
doi:10.1016/j.egypro.2014.03.241

1. Introduction

Concentrating Solar Power (CSP) Plants have the best technology available to make possible the conversion and exploitation of the sun energy due to their ability to adapt their production to electricity grid requirements thanks to their storage systems. However, CSP plants have some challenges related with the weather forecast and the presence of clouds, both of which affect the thermal production. Therefore, it seems logical to conduct an exhaustive study of cloud cover and forecast for an efficient management of CSP plants.

The use of satellite images for weather forecasting is one of the most widespread and used techniques. Chiefly, these images have been useful to study solar radiation in different places around the world. Janjai et al. (2009) [1] derived global hourly solar radiation from the visible channel of the Geosynchronous Meteorological Satellite 5 (GMS-5) satellite, while Şenkal and Kuleli [2] utilized Meteosat imagery together with Artificial Neural Networks (ANNs) for the estimation of solar radiation in Turkey. For their part, Zarzalejo et al. (2005) [3] developed a model based on ANNs to quantify the influence of the satellite detected clouds on hourly solar irradiation. More recently, Şenkal (2010) [4] used remote sensing and ANNs to predict global solar radiation without any meteorological data and with a relatively good connection between measures and predicted values. Also, the cloudiness has been analyzed through the use of satellite images. Ghosh et al. (2006) [5] applied certain rules to METEOSAT-5 satellite images to study three different types of cloud coverage: overcast, partially covered and cloudless. One further step has been taken by Escrig et al. (2013) [6], where satellite imagery has been used to do a classification of clouds.

Due to the resolution limitations of satellite images -which are unable to predict small clouds in the sky-, hemispheric sky cameras (fisheye lens) are the most suitable technology to study the cloudiness from a ground vision. Sabburg and Wong (1999) [7] analyzed whether the solar disk in sky images is blocked by clouds by using a lineal algorithm applied to images obtained with a sky camera, and comparing the results with human observations. Later, Kassianov et al. (2005) [8] developed a model to study the cloudiness coverage using a TSI camera (Total Sky Imager). Long et al. (2006) [9] did a characterization of clouds, but they encountered a problem in the classification of the Sun area: they mistakenly classified this zone as cloud or sky one. Largely, the saturation comes from aerosol loading, thin cirrus clouds or haze. Solar altitude was employed to establish that in low solar altitudes, the problem appears more frequently. Olmo et al. (2008) [10] presented a model to retrieve the optical depth of the aerosols using images from a sky camera when Sahara dust and aerosol load are analyzed. In 2011, Martínez-Chico et al. [11] presented a model where a classification of clouds was done with images from a sky camera (TSI-880). In this work, direct solar radiation was required to observe the occurrence of clouds classified in four groups, allowing a possible study of the attenuation of direct solar radiation depending on the type of cloud.

The aim of this work is to present a methodology and an interactive portal able to make a short and medium-term forecast in real-time using MSG and sky camera (TSI-880 model) imagery and radiometric data.

2. Data

The methodology explained below employs Meteosat Second Generation (MSG) imagery. MSG satellite takes earth's pictures every 15 minutes in 11 spectral channels with a 3 km resolution. The images from a sky camera (TSI-880 model) are taken every minute with 352x288 color-pixels resolution divided in the three channels of the RGB color space, and the diffuse, direct and global irradiance which are taken with the same frequency.

Throughout this project we have chosen and analyzed images from all possible types of skies, from the earliest moments of the day till the latest just before the sunset, and from different times of the year. The total studied period covers from 2010 to 2012, including the modeling and testing stages. For the modeling part, we have used data from 2010 till 2012; and for the testing part, we have chosen two different locations: University of Almería (Almería, Spain) and Gemasolar Plant (Fuentes de Andalucía, Spain) during 2010 and 2011. The TSI images can be only collected when the solar altitude is above 5º and for MSG images when it is above 10º.

3. Methodology

In this section we will be briefly introduce the methodology used to make the cloudiness forecasting for short and medium-term periods using MSG and TSI images along with radiometric data, with the purpose of generating useful information for the operators of CSP Plants.

3.1. Clouds detection in MSG imagery

Due to the specific situation of the MSG Satellite, its vision of clouds can only inform us about the highest portion of the clouds. Therefore, if there is a situation where there are clouds at different layers, the MSG Satellite can only study the highest ones. Despite this, the MSG is a potential tool to study atmospheric phenomena over time. In the present work, cloud detection is conducted using five channels (VIS 0.6, VIS 0.8, IR 3.9, IR 10.9 and IR12.0). The first step consists of converting each pixel from a grey level to radiances in accordance with MSG calibration parameters. After that, depending on the wavelength of the channel, different tests are applied to each pixel. A snow detection test has been used prior to the other test to avoid misclassification of bright cold snowy clouds, Derrien and Le Gléau (2010) [12]. Infrared - visible channel ratio test [9], emissivity difference test [13, 12] and spatial texture test [14], have been used according to their specifications in order to improve cloud detection. Using this as our starting point, an albedo map for cloudless pixels for each month has been defined to compare the value of each reflectance with the corresponding map for detecting cover pixels. Also, an infrared temperature threshold test has been used to determine the temperature of pixels in order to determine the presence or absence of clouds in the analyzed pixel. Finally, the detection of clouds allows us to have an accurate model that can be used to identify whether or not the pixel with the desired location is covered by clouds.

3.2. Clouds motion using MSG imagery

As a complement of the above, a specific model has been developed to follow the trajectory of clouds using images from MSG Satellite. For having a better understanding of clouds motion, clouds are classified as low, medium and high by the latitude criterion from Stowe et al. (1988) [15].

Satellite image is further divided into five horizontal sectors defined around the place of study. Four rectangular sectors are obtained by dividing the image along its two bisections. The fifth sector has the same shape and size as the previous ones, but centered in the middle of the image. Figure 1 shows the different sectors.

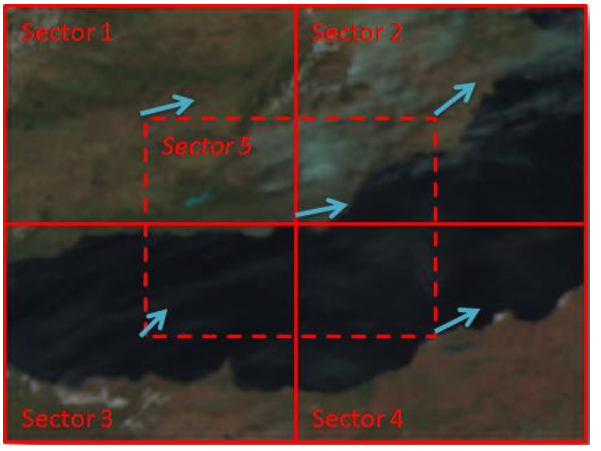

Figure 1. - Sectors of an image from MSG satellite

Thus 15 binary matrices (cloud/cloud-free pixel) are generated for one raster image.

In the analysis of the clouds motion, three consecutive images are taken from the MSG satellite. Then, through the method of binary cross correlation and different coherence tests, it is possible to obtain the clouds motion of each sector. After that, each sector is moved according to the vectors obtained by estimating the cloudiness for short and medium term (3 hours). The cloud movement will be estimated once every 15 minutes (the time spent between two consecutive images).

3.3. Clouds detection in TSI-880 images

Images from sky camera (fisheye lens) are taken every minute, as it is the best frequency to do so due to the constant changes that happen in the atmosphere. For the successful detection of clouds in the images it is necessary to process the three channels that make up the image. Additionally, each image is transformed in the HSV color space, having a total of six different channels for detecting the clouds. After testing, we faced some difficulties, such as the saturation of pixels in the sun area, which made it clear the necessity of using another variable that could improve the model. In this case, a radiometric variable was selected as the most useful tool to solve those problems.

3.3.1. Use of radiometric data

The presence of clouds has a direct relationship to radiometric variables. Thus, values from pyranometers (diffuse and global components) and pyrheliometer (direct component) were taken to establish a classification of sky conditions as observed in the TSI images. This classification determines whether the sun is cloudless, partially cloudy or overcast (the same categories indicated for the MSG Imagery). Also, an estimation of diffuse, direct and global radiation has been conducted for the improvement of the classification.

Therefore, based on this classification, the re-processing of images is carried out. As there are three different classifications, there are three different models to process images. This processing of images is performed by determining relations between the channels of the RGB and HSV color spaces. The result is an image with the same length than the original image, and which perfectly represents this original image, identifying the clouds.

3.4. Clouds motion using TSI-880 images

In regards to the clouds motion, three consecutive images from TSI-880 sky camera are taken to study the evolution of clouds from a ground vision (one each minute). In this case, clouds are not classified as low, medium or high as it is not possible to calculate the height of the clouds with just one camera.

Due to the curvature of the dome of a sky camera, the clouds which appear in the borders of the images have a lower motion than the clouds that appear in the center. This effect is so because the pixels in the border of the camera represent a bigger portion of the sky (the horizon). Figure 2 shows the sectors in which the image is divided to study the motion of clouds. A total of 23 sectors were established in view of the spherical geometry of the camera.

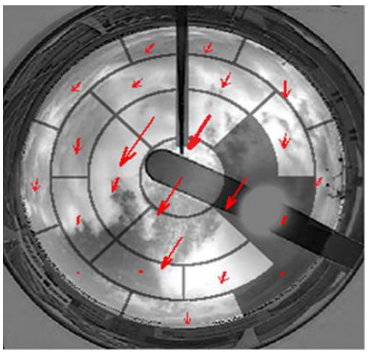

Figure 2. - Sectors defined in an image of the TSI-880 sky camera

For each sector, the clouds motion is analyzed through different tests (spatial, temporal and final coherence) to check that the movement is correct. These tests are designed to avoid misclassifications of the vectors, having as a result the displacement which must be applied to each sector to forecast clouds motion. In our case, we will be processing 30 displacements of the clouds (for a forecast of 30 minutes) to find if there are instances when clouds may be blocking the sunlight.

3.5. Interactive portal – application to the CSP plant operation

To give a joint view of all the methodologies explained before and to offer the CSP plants Operators an easy and intuitive application, an interactive portal has been designed to collect the steps and procedures required for a real-time forecast updated every minute.

The application has been developed using the Matlab development environment, as it is one of the best complex processing and long operations with matrixes tools and for its ability to generate a user-friendly interface. Figure 3 shows the user interface of the application.

The application starts by retrieving the information of radiation data and images from the MSG satellite and TSI-880 camera. The recovering time is precisely 50 minutes as it is the exact amount of time needed to get the last three images off the satellite (15 minutes for each one) in order to make the first medium-term forecast (3 hours). Also, radiation data and images from sky camera are taken to be shown in the application. Then, while in offline mode, the images from TSI-880 camera are taken with the same purpose as the satellite images but for making the first 30 minutes forecast. The historical file of radiation (the three radiation components) of the whole day is retrieved from a file updated and stored every minute in a server which manages and stores both images as well as the radiation components.

The satellite images are retrieved in a compressed format. Then, using an external application (installed in the server which receives the original images), the raw images are decompressed and cut, putting together the final images in Matlab format with the clipping of the desired place. This process is repeated until the offline time matches the current time, and from here on out the application switches back to online mode to continue the execution of operations.

Focusing now in the description of the interactive portal, the user-friendly interface is divided in five parts: the first one is the left part of the screen, where the DNI evolution is shown; the second one in the middle of the screen shows the area dedicated to the MSG images; the third part is located in the right side of the figure and depicts the images of the sky camera (fisheye lens); the last two areas are located below the ones already mentioned: the one on top is designed to display the short and medium-term forecast (from 1 minute till 3 hours) while the some at the bottom provides relevant information about internal processes.

The first block, which as stated is on the left side of the screen, displays different items. At the top, we see the date ('dd-mmm-yyyy' format) and the civil time ('hh:mm' format), both of which are updated every minute. Underneath there is an area allocated to direct normal irradiance. It comprises three elements that inform the operators of the evolution of radiation throughout the day. Firstly, the last value of radiation (in W/m^2) is shown in a text box. This value is incorporated into the blue colored graph as a singular connotation (a red circle around a blue point). The graph has two axes representing direct normal irradiance (from 0 to 1000 W/m^2, in intervals of 200 W/m^2) vs. civil time (from 00:00 to 23:59). Finally, in the top-left part of the graph there is a box with a fill color. This color serves as an indicator to the operators to let them know whether or not there is a delay in the reception of radiometric data. The color green (as in the example) indicates that there is no delay in the reception of direct normal irradiance; meanwhile, a yellow box shows that there is a delay of one minute, whereas the red color filling the box means that the last value of direct normal irradiance was taken 2 or more minutes ago. This graph is originated only when the value of solar altitude is higher than 0º, because bellow this measure the values of radiation are 0 W/m^2. Internally, diffuse and global radiation measurements are taken.

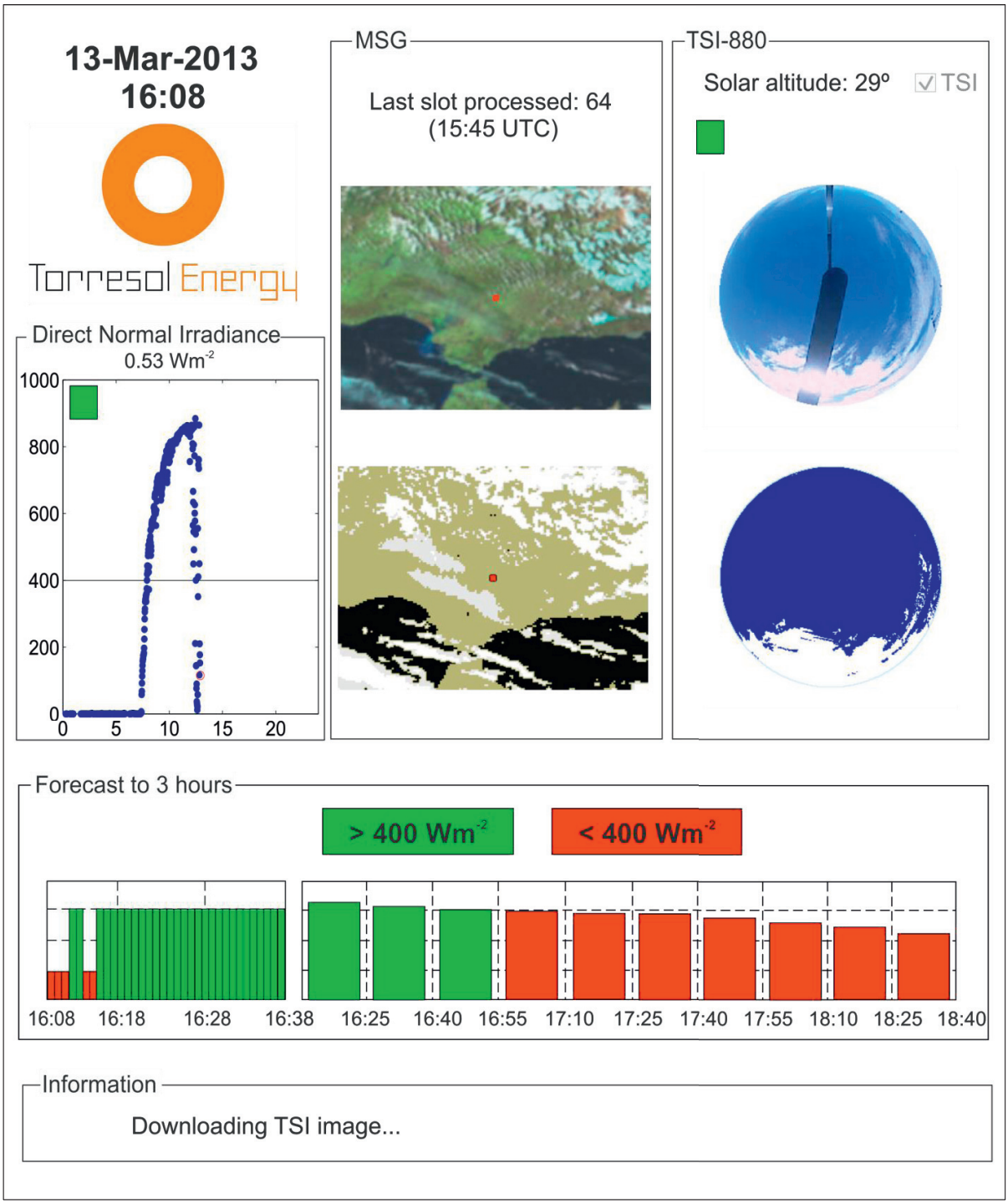

Figure 3. - Display of the interface for prediction of cloudiness placed in Gemasolar

The second part above mentioned is located in the middle vertical section of the screen. This area has been developed for satellite images. At the top of this area there is a text box showing a time stamp of the last image received from MSG satellite and a number that represents the order of this image (one every 15 minutes starting at

00:00 hours). Under this text box a video containing the last 2 hours of images is uploaded, showing the evolution of clouds in that time. Each image is a composition of three channels: VIS0.6, VIS0.8 and IR1.6 (the numbers express the wavelength in μm) forming a false color representing the vision of satellite in an understanding way. The sequence of these images provides enough information to CSP Plants operator as to allow them to check the trajectory of clouds in real time. Under this composition from MSG satellite imagery, the processed images are presented, reproduced in the same sequence and showing the identification of clouds as a result of applying the methodology described in the section 3.1. This system starts to operate when the solar altitude angle is higher than 10º.

The area reserved to the TSI images is the one located on the right side of the interactive portal. Firstly, located at the top of this section there is a text box with periodically updated information of the solar altitude angle expressed as an integer. On its right there is a check box which is refreshed automatically when a new image is received. Also, as was the case with the radiometric data, there is a box filled with different colors right beneath the information on solar altitude. A green color filling the box indicates that at present there is no delay in the reception of images from the sky camera ; a yellow color informs of the existence of a delay of one minute, while that the presence of red in the box means that the last image was taken 2 or more minutes ago. In regards to the first picture which can be found in this area, it shows a sequence of 10 consecutive images displaying the sky conditions present during the last ten minutes. Underneath this sequence, the processed images are displayed for the same interval. In the processed images the support of the camera and the shade band are removed to avoid misclassification of pixels. In this way, it is possible to check if the processed images represent the original ones accurately as thus to ensure that the model has not any errors. For its part, this section starts to operate when solar altitude is higher than 5º, providing the short-term forecast for the next 30 minutes.

Next on the explanation of the different parts of the portal is the fourth section, which has been exclusively design to illustrate the short and medium-term forecast of cloudiness to predict future situations of sky conditions. In an informative way, there are two boxes at the top (keys) which inform of the colors chosen to establish when there will be a direct normal irradiance higher than 400 W/m^2 (green color) and when it is lower than 400 W/m^2 (red color) (this is a threshold value that corresponds to the optimal irradiance indicated to operate a central tower plant). These boxes give two different forecasts: the first one is focused on the prediction using TSI-880 images, while the second one is focused on the prediction using satellite images. As shown in Figure 3, the first forecast starts with thin bars corresponding to the 3o minutes forecast (using the three consecutive TSI images). When the forecast determines that there will be clouds in the next period, the height of the bar shortens and turns to red. On the other hand, if the forecast informs that in the next minutes the sky will be free of clouds, the length of the bars lengthens and turn to a green color. The second forecast, which corresponds to the 3 hours forecast (using images from MSG satellite), has the widest bars. In this case, the decreasing height of bars in the prediction does not add extra information to the operators. The color of bars will be red when the forecast establishes that in the near future there will be clouds in some interval of time, whereas the bar will be green when the forecast informs that the sky will be clear of clouds.

Finally, the last block located at the bottom of the interface is designed to give useful information about the internal processes which the program is running. Internal process like "Downloading a TSI-880 image", "Downloading radiation data", etc. provide the operator with the necessary details to know in which status is the application.

The application never stops thanks to the embedded algorithm, and it is updated periodically (normally every 10-15 seconds). At the same time, all the data is stored within the computer where the application may be running at the time for future analysis and evaluations. If while the application is running a problem occurs (e.g., there is no synchronization between radiation data and sky camera images, an image from the satellite is lost, etc.) the program keeps running without any interruption and once troubleshooted, the application continues making forecasts without mistake.

4. Results

The evaluation of the application has been done after running the software for two consecutive years (2010 and 2011) to observe the accuracy of the forecast, using the images from the sky camera (TSI-880 model) and the images from MSG satellite. The process carried out to check the model consists of comparing the forecast made by both tools (MSG and TSI images) with the real values of direct normal irradiance of preestablished moments in two different places (as it was indicated in the Section 2), University of Almería (Almería, Spain) and Gemasolar Plant (Fuentes de Andalucía, Spain). The application predictive ability is considered to be successful (for both tools) if the prediction establishes that there are clouds and the radiation is lower than 400 W/m^2, and when the prediction establishes that there are not clouds and the radiation is over 400 W/m^2.

Figure 4 shows the success of the forecast for a medium-term period (3 hours) using the two technologies.

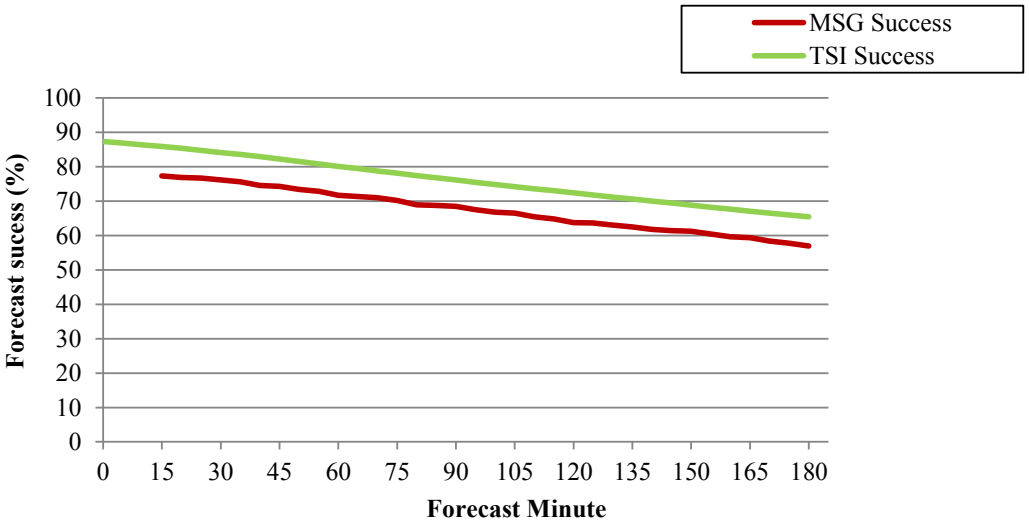

Figure 4. - Success of MSG and TSI-880 forecast

While analyzing Figure 4, it is noticeable that the forecast performed with TSI-880 images has a higher success than the one performed using MSG satellite images because the accuracy with a ground vision is higher than the resolution of satellite pixels. However, in the interactive portal during the first thirty minutes the forecast made with TSI imagery is the one being used because, as it has been previously stated, it has a higher accuracy rate than MSG images; nevertheless, the illustration depicted only comprises this time frame because in many occasions is not possible (with a TSI-880 camera) to make a forecast more than thirty minutes in advanced due to the limitations of this sky camera to see beyond its field of view. As such, in these occasions it is not possible to identify futures clouds motions.

For both technologies, the forecast success decreases as time goes by due to the changes that clouds may experience, which can modify their form and motion after a while.

In the case of the forecast made using images from sky camera (TSI-880 model), the forecast has a success rate in the first minute higher than 87%. In the fifth minute, the success value remains close to 87%. The forecast accuracy in minute 15 is a bit below 86%, whereas in minute 30 the forecast has a probability of success of approximately 84%. From minute 30 on to the last forecast (three hours) the success decreases at a constant rate. The TSI camera forecasts made from more than thirty minutes in advanced are usually for cloudless skies, when the forecasts are less relevant and there are no motions to analyze. That is why as a rule we will use the MSG satellite forecast for predictions beyond 30 minutes.

If we were to check for errors by comparing the forecast made with MSG satellite images to the direct normal irradiance, the data thus obtained would tell us that for the first prediction (15 minutes) the average success for the

two years analyzed is close to 78%, similar to that of minute 30. One hour forecasts have an average rate of success of 72%. For forecasts into the near future (medium-term) the decreasing line of success has a similar trend than the TSI-880 forecast line, showing the impact that atmospheric conditions may have and the difficulties that they can present. Nonetheless, this information is very important and transcendental in order to be able to foretell clouds motions with sufficient time and to adapt the operations of the CSP Plants to the forecasted changes.

5. Conclusions

With the purpose of getting ahead of future events in the atmosphere which can affect the management of CSP Plants, an interactive portal has been developed which offers a short to medium-term forecast of cloudiness in real-time.

The benefits of this portal lay primarily in the optimization and in the maximization of the performance of the thermal production, thanks to the helpful information that the website offers for future clouds movements, which helps operators take the most appropriate decisions while operating their plants.

Two different forecasts have been presented: the first one a forecast into the first thirty minutes (from input time) using images from a sky camera (model TSI-880), and the second one a forecast three hours into the future using images from the MSG satellite. The application is updated every 10-15 seconds, providing operators with constantly updated information.

The rate of success of the forecast made using a sky camera varies from 87 to 84% for forecasts from one to thirty minutes into the future. Forecasts over that mark are faced with the limitation of fisheye cameras whereby if there is a presence of clouds, it is not possible to make displacements predictions in those times. Therefore, in the application we have developed TSI camera forecast is only used for the first thirty minutes.

For the forecast based on MSG satellite images, for predictions one hour into the future the success rate is approximately 72%, offering a good accuracy for the cloudiness forecast. With this technology, the limitation of sky cameras does not apply because it is possible to have a higher vision than using images from said sky cameras.

Traditional images from satellite have been contrasted with ground views for the study of cloudiness, giving a high accuracy of the short and medium-term forecast using ground views.

Thus, the application we have developed (with its correspondent user-friendly interface) signifies a new step in improving the management of CSP Plants as it helps to have a better knowledge of future meteorological phenomena in the atmosphere; with this tool it is possible to establish a better operation mode for a higher production in these kind of solar power plants.

Acknowledgements

This project has been financed by Torresol Energy Investments, S.A., to which we wish to acknowledge their collaboration, and especially to Gemasolar Plant. Also, the authors wish to acknowledge the CDTI (IDI-20091384) and the project (CGL2011-30377-C02-02) that was funded by the Ministerio de Economía y Competitividad.

References

[1] Janjai S, Pankaew P, Laksanaboonsong J. A model for calculating hourly global solar radiation from satellite data in the tropics. Applied Energy 2009;86(9):1450-7.

[2] Şenkal O, Kuleli T. Estimation of solar radiation over Turkey using artificial neural network and satellite data. Applied Energy 2009;86(7-8):1222-8.

[3] Zarzalejo LF, Ramírez L, Polo J. Artificial intelligence techniques applied to hourly global irradiance estimation from satellite-derived cloud index. Energy 2005;30:1685-97.

[4] Şenkal O. Modeling of solar radiation using remote sensing and artificial neural network in turkey. Energy 2010;35:4795-801.

[5] Ghosh A, Pal NR, Das J. A fuzzy rule based approach to cloud cover estimation. Remote Sensing of Environment 2006;100:531-49.

[6] Escrig H, Batlles FJ, Alonso J, Baena FM, Bosch JL, Salbidegoitia IB, et al. Cloud detection, classification and motion estimation using geostationary satellite imagery for cloud cover forecast. Energy 2013; Http://dx.doi.org/10.1016/j.energy.2013.01.054.

[7] Sabburg J, Wong J. Validation of improved sky camera algorithm for measurement of cloud around the sun; 1999. Queensland University of Technology.
[8] Kassianov EI, Long CN, Ovtchinnikov M. Cloud sky cover versus cloud fraction: Whole-sky simulations and observations. Journal of Applied Meteorology 2005;44:86-98.
[9] Long CN, Sabburg JM, Calbó J, Pagès D. Retrieving cloud characteristics from ground-based daytime color all-sky images. Journal of Atmospheric Ocean Technology 2006;23:633-52.
[10] Olmo FJ, Cazorla A, Alados-Arboledas L, López- Álvarez MA, Hernández-Andrés J, Romero J. Retrieval of the optical depth using an all-sky CCD camera. Applied Optics 2008;47:182-9.
[11] Martínez-Chico M, Batlles FJ, Bosch JL. Cloud classification in a mediterranean location using radiation data and sky images. Energy 2011;36:4055-62.
[12] Derrien M, Le Gléau H. Algorithm theoretical basis document for "Cloud products" (CMa-PGE01 v3.0, CT-PGE02 v2.0 & CTTH-PGE03 v2.1). Available online; 2010.
[13] Saunders RW, Kriebel KT. An improved method for detecting clear sky and cloudy radiances from AVHRR data. International Journal of Remote Sensing 1988;9(1):123-50.
[14] Derrien M, Le Gléau H. MSG/SEVIRI cloud mask and type from SAFNWC. International Journal of Remote Sensing 2005;26(21):4707-32.
[15] Stowe LL, Wellemeyer CG, Yeh HYM, Eck TF. Nimbus-7 global cloud climatology. part I: Algorithms and validation. Journal of Climate 1988;1(5):445-70.